Effective exchange fields in spin-torque resonance of magnetic insulators

Chiba, T; Bauer, GEW; Takahashi, S

DOI
10.1016/j.jmmm.2015.07.058

Publication date
2016

Document Version
Final published version

Published in
Journal of Magnetism and Magnetic Materials

Journal of Magnetism and Magnetic Materials 400 (2016) 163–167

Contents lists available at ScienceDirect

Journal of Magnetism and Magnetic Materials

journal homepage: www.elsevier.com/locate/jmmm

Effective exchange fields in spin-torque resonance of magnetic insulators

Takahiro Chiba [a,*], Gerrit E.W. Bauer [a,b,c], Saburo Takahashi [a]

[a] Institute for Materials Research, Tohoku University, Sendai 980-8577, Japan
[b] WPI-AIMR, Tohoku University, Sendai, Miyagi 980-8577, Japan
[c] Kavli Institute of NanoScience, Delft University of Technology, Lorentzweg 1, 2628 CJ Delft, The Netherlands

ARTICLE INFO

Article history:
Received 20 June 2015
Received in revised form
17 July 2015
Accepted 18 July 2015
Available online 20 July 2015

Keywords:
Yttrium iron garnet
Spin-torque ferromagnetic resonance
Spin-Hall magnetoresistance
Spin-mixing conductance

ABSTRACT

We report additional results on the spin-torque ferromagnetic resonance (ST-FMR) of a bilayer system made from a magnetic insulator such as $Y_3Fe_5O_{12}$ (YIG) and a heavy normal metal such as Pt in terms of the interface spin-mixing conductance and including spin pumping. We analyze experimental ST-FMR spectra for out-of-plane and in-plane magnetization configurations in terms of an anisotropic imaginary part G_i of the mixing conductance (or interface effective field). The estimated ratio between imaginary and real parts $G_i/G_r \lesssim 0.3$ is sensitive to an (unknown) phase shift between microwave current bias and associated Oersted field.

1. Introduction

The ferrimagnetic insulator (FI) $Y_3Fe_5O_{12}$ (YIG) can be electrically [1] and thermally [2] activated by attached heavy normal metals (NM) such as Pt with large spin Hall angle. We proposed to employ spin-torque ferromagnetic resonance (ST-FMR) [3,4] to study magnetic insulators [5,6] by making use of the spin Hall magnetoresistance (SMR) [7,8] (see Fig. 1). Iguchi et al. [9] reported negligibly small effects due to SMR when subjecting a YIG‖Pt bilayer to FMR conditions in a microwave cavity. On the other hand, Schreier et al. [10] and Sklenar et al. [11] do find SMR rectification voltages when driving a microwave current through the Pt. The first collaboration interprets the differences of the observed spectra in samples with different thicknesses of both Pt and YIG in terms of the competition between Oersted fields, spin–orbit torques, and spin pumping [10], in good agreement with theoretical predictions [5]. The second group focuses on the ST-FMR measurement in out-of-plane (oop) magnetization configurations and reports a SMR rectification that is affected by an additional effective field [11].

The spin transport through the interface between ferromagnets and normal-metals is governed by the complex spin-mixing conductance $G^{\uparrow\downarrow} = G_r + iG_i$ (per unit area of the interface) [12]. The predicted large G_r for the interfaces between YIG and simple metals [13] has been confirmed by experiments [14,15]. G_i can be interpreted as an effective exchange field between magnetization and a spin accumulation in an attached NM, which in the absence of spin–orbit interaction is usually much smaller than the real part. However, field-like spin–orbit torques have been found in metallic structures [16,17]. In the YIG|Pt system the SMR for out-of-plane magnetizations has been interpreted in terms of a $G_i \ll G_r$ [18,19].

Here we compute ST-FMR signals of ferro- or ferrimagnetic insulators attached to a heavy normal metal by modeling a field-like torque (including ac spin pumping contributions) allowing for a large $|G_i|$ [6]. In Ref. [10] the phase between Oersted field and applied microwave current was assumed to suffer a phase shift due to unknown origins. We show that the experiments with an adjustable phase can be also explained by introducing an anisotropic interface field-like torque. We fit the observed frequency-dependent voltages [10] for nearly perpendicular and in-plane magnetization configurations in terms of an adjustable G_i for an ultra thin film of YIG. We find an anisotropic G_i that is larger for the out-of-plane than the in-plane magnetization configuration, which is still smaller than the real part G_r, however. The sizable G_i (of the order of G_r) reported for mostly out-of-plane magnetization configurations [11] is qualitatively consistent with our results.

2. Spin-torque ferromagnetic resonance

The ST-FMR technique should be distinguished from the electrical (inverse spin Hall effect) detection of conventional FMR in

* Corresponding author.
E-mail address: t.chiba@imr.tohoku.ac.jp (T. Chiba).

http://dx.doi.org/10.1016/j.jmmm.2015.07.058
0304-8853/

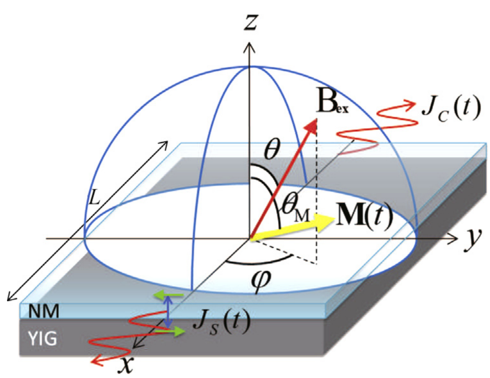

Fig. 1. Schematic of the device to observe the SMR rectified voltage in which an external magnetic field $\mathbf{B}_{\rm ex}$ is applied to the direction characterized by a polar angle θ and a azimuth φ while $\theta_{\rm M}$ shows the magnetization angles. The YIG(d_F nm)|N(d_N nm) bilayer film is patterned into a strip with a length L.

which the magnetization dynamics is excited by microwaves in coplanar wave guides or cavities. The ST-FMR magnetization is excited by spin Hall spin currents generated by an ac electric current bias (although Oersted magnetic fields may not be disregarded). An external magnetic field $\mathbf{B}_{\rm ex}$ is described by a polar angle θ and azimuth φ in the x–y plane. The magnetization dynamics can be expressed by the Landau–Lifshitz–Gilbert (LLG) equation with interface torques [5],

$$\partial_t \hat{\mathbf{M}} = -\gamma \hat{\mathbf{M}} \times \left(\mathbf{B}_{\rm eff} + \mathbf{b}_{\rm Oe}(t)\right) + \alpha \hat{\mathbf{M}} \times \partial_t \hat{\mathbf{M}} + \boldsymbol{\tau}_{ST}(t), \tag{1}$$

where $\mathbf{B}_{\rm eff} = \mathbf{B}_{\rm ex} + \mathbf{B}_{\rm dm} + \mathbf{B}_{\rm sm}(t)$ consists of the external magnetic field, the static demagnetizing field, and the dynamic demagnetization field, respectively. The Oersted field from the microwave current $\mathbf{b}_{\rm Oe}(t) = \mathbf{b}_{\rm Oe} e^{i(\omega_a t + \delta)}$ with frequency $\omega_a = 2\pi f_a$ and magnitude is determined by Ampère's Law (in the limit of an extended film) $b_{\rm Oe} = \mu_0 J_c^0 d_N/2$, where $J_c{}^0$ is an applied charge current density and δ the phase shift between Oersted field and current that is governed by the details of the sample design and therefore treated as an adjustable parameter [20]. The current-induced effective field generates the torque

$$\boldsymbol{\tau}_{ST}(t) = \gamma\left(b^r_{ST}\hat{\mathbf{M}} \times \hat{\mathbf{M}} \times \hat{\mathbf{s}} + b^i_{ST}\hat{\mathbf{M}} \times \hat{\mathbf{s}}\right)e^{i\omega_a t}, \tag{2a}$$

$$b^{r(i)}_{ST} = \frac{\hbar}{2|e|\mu_0 M_s d_F}\,\mathrm{Re}\left(\mathrm{Im}\right)\left[\eta\right]\theta_{\rm SH} J_c^0, \tag{2b}$$

where M_s and d_F are the saturation magnetization and thickness of the FI film, $\theta_{\rm SH}$ and $\hat{\mathbf{s}}$ the spin Hall angle and the direction (a unit vector) of the injected spin moment, and η the complex spin diffusion efficiency $\eta = g_S \tanh[d_N/(2\lambda)]/\left(1 + g_S \coth(d_N/\lambda)\right)$ with

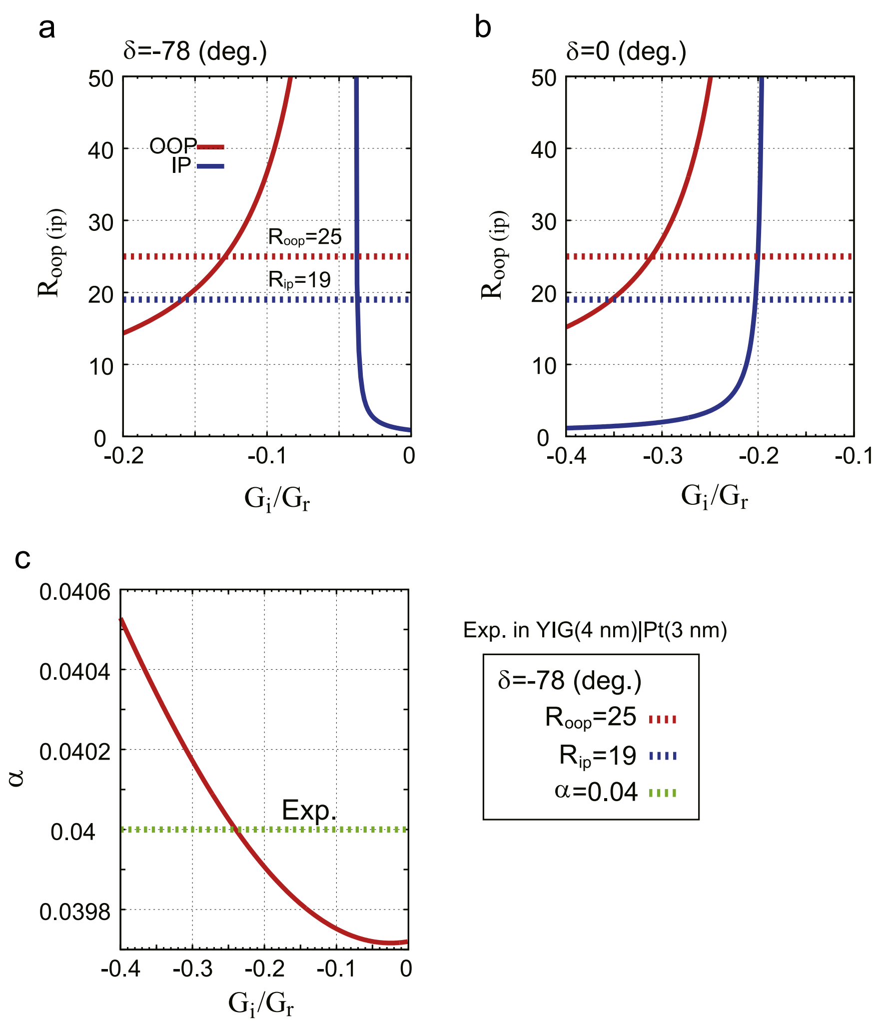

Fig. 2. (a)(b) The ratios of symmetric and antisymmetric contributions to the dc voltage for out-of-plane and in-plane magnetizations as a function of the G_i for (a) $\delta = -78°$ and (b) $\delta = 0°$. (c) The magnetization damping parameter α as a function of G_i. Dashed horizontal lines represent the experimental values for YIG(4 nm)|Pt(3 nm) [10]. $G_r = 4.0 \times 10^{14}\ \Omega^{-1}\,\mathrm{m}^{-2}$, $M_s = 128$ kA/m, $\gamma_0 = 1.76 \times 10^{11}\ \mathrm{T}^{-1}\,\mathrm{s}^{-1}$, $\alpha_0 = 8.58 \times 10^{-5}$ [21], $\theta_{\rm SH} = 0.11$, $\lambda = 1.5$ nm, and $\rho = 48.1\ \mu\Omega$ cm at $f_a = 7$ GHz are used for plotting.

$g_S = 2\lambda\rho G^{\uparrow\downarrow}$, λ the spin-diffusion length, and ρ the resistivity of bulk NM. γ and α are the modulated gyromagnetic ratio and magnetization damping by the spin pumping in terms of the intrinsic values γ_0 and α_0, expressing $\gamma = \gamma_0/\left(1 - \alpha_1 \coth[d_N/(2\lambda)] \text{ Im } \eta\right)$ and

$$\alpha = \frac{\alpha_0 + \alpha_1 \coth\left(\frac{d_N}{2\lambda}\right) \text{Re } \eta}{1 - \alpha_1 \coth\left(\frac{d_N}{2\lambda}\right) \text{Im } \eta} \tag{3}$$

with $\alpha_1 = \gamma\hbar^2/(4\lambda\rho e^2\mu_0 M_s d_F)$.

In the ST-FMR experiment, the dc voltage arises from not only the mixing of applied microwave currents and the oscillating SMR in NM (spin rectification or spin torque diode effect) but also the ISHE mediated via spin pumping (see Appendix A). Let us discuss about the out-of-plane magnetization configuration which has a possibility to detect the as yet unknown spin–orbit induced torques or a finite imaginary part of the spin-mixing conductance to magnetic insulators [11]. In the out-of-plane configuration the voltage $V_{\text{SMR}}^{\text{II}} - V_{\text{SP}}^{\text{II}} = S^{\text{II}} F_S(B) + A^{\text{II}} F_A(B)$ in Eqs. (A.2b) and (A.3b) is the only observable (setting $\varphi = \pi/2$). The ratio between symmetric and antisymmetric components is defined by

$$\text{R}_{\text{oop}} = \frac{S^{\text{II}}}{A^{\text{II}}} = \frac{\sin \delta + CR_r/C_-}{\cos \delta + R_i} - \frac{\nu_{\text{SP}}}{\nu_{\text{SMR}}}\frac{\gamma h_{Oe}}{\alpha\omega_a} C \frac{1 + 2R_i \cos \delta + R_i^2 + C_+ R_r^2/C_- + 2CR_r \sin \delta/C_-}{\cos \delta + R_i}, \tag{4}$$

where $R_{r(i)} = b_{ST}^{r(i)}/b_{Oe} = \Phi_0 \text{ Re}\left[\eta\right]\theta_{\text{SH}}/\left(\pi\mu_0 M_s d_F d_N\right)$ with flux quantum Φ_0 and vacuum permeability μ_0. The calculated ratio is plotted in Fig. 2 as a function of G_i and δ for the YIG|Pt material parameters [10]. For reference, we plot the same ratio for an in-plane magnetization as defined by $\text{R}_{\text{ip}} = S^{\text{I}}/A^{\text{I}}$ and a voltage $V_{\text{SMR}}^{\text{I}} - V_{\text{SP}}^{\text{I}} = S^{\text{I}} F_S(B) + A^{\text{I}} F_A(B)$ in Eqs. (A.2a) and (A.3a). These ratios (and dc voltages itself) sensitively depend on the YIG thickness since the spin transfer torque $b_{ST}^{r(i)}$ is proportional to $1/d_F$ and spin pumping dominates the FMR linewidth due to the low magnetic damping of YIG. The torques become clearly observable only for very thin YIG films [10]. In Fig. 2(a) and (b), the calculated ratios are compared with the experimental ones [10], which show that G_i is negative. The crossing points determine our estimate for the imaginary part of the spin-mixing conductance as displayed in Table 1. The imaginary parts are larger for out-of-plane than in-plane magnetizations, which is possible only in the presence of significant spin–orbit interactions. The results are qualitatively consistent with Ref. [11] although our $\left|G_i\right| \le 0.3G_r$ as not as dominant. The magnetization damping equation (3) in Fig. 2 (c) also narrows down G_i to roughly 24% of the real parts irrespective of the phase, but this value is obtained assuming isotropic damping.

Table 1
Estimates for $|G_i|$ in units of $10^{14}\ \Omega^{-1}\text{m}^{-2}$ for two values of the phase between ac current and Oersted field. The value in the lower row is obtained from fitting $|G_i|$ to an isotropic Gilbert damping.

Imaginary part of the mixing conductance	$\theta=5°$	$\theta=90°$
$\delta=-78°$	0.52	0.15
$\delta=0°$	1.25	0.81
α	0.96	0.96

3. Effect of SMR rectified ac spin pumping

When the magnetization in the ferromagnetic – insulator |normal – metal junction is excited, the spin pumping leads to the injection of pure spin currents into the normal metal. The pumped spin current has a large polarization of time-dependent ac components compared to a dc component [22–26]. Here we evaluate a dc-signal due to the ac components of the pumped spin currents via SMR driven spin rectification. The spin pumping-induced charge current is [5]

$$\begin{aligned} J_{\text{SP}}(t) &= -J_r^P \omega_a^{-1}\left(\hat{\mathbf{M}} \times \partial_t \hat{\mathbf{M}}\right)_y - J_i^P \omega_a^{-1}\partial_t \hat{M}_y \\ &= J_{\text{SP}}^{(0)} + J_{\text{SP}}^{(\omega a)}(t) + J_{\text{SP}}^{(2\omega a)}(t), \end{aligned} \tag{5}$$

where $J_{\text{SP}}^{(0)}$ is an ordinary dc component, and $J_{\text{SP}}^{(\omega a)}(t)$ and $J_{\text{SP}}^{(2\omega a)}(t)$ are time-dependent ac components with frequencies ω_a and $2\omega_a$, respectively, and $J_{r(i)}^P = \hbar\omega_a/(2|e|d_N\rho)\theta_{\text{SH}} \text{ Re}\left(\text{Im}\right)\left[\eta\right]$. The ISHE ac current due to the ac spin pumping is rectified through mixing of the oscillating SMR to give an additional dc-signal with a different dependence of the ST-FMR signal on the field angles. This effect (ac-SP rectification) can be also caused by the modulation of the resistance (ρ_{xx} [8,9,5]) times the spin pumping induced ac current component, that is,

$$\begin{aligned} V_{\text{SMR}}^{\text{ac}} &= L\left\langle \rho_{xx}[\hat{M}_y^2(t)]J_c^{(\omega a)}(t)\right\rangle_t \\ &= -V_{\text{SMR}}^{\text{ac,I}} \cos \varphi \sin 2\varphi\left(1 - \sin^2 \varphi \sin^2 \theta_{\text{M}}\right) \sin \theta_{\text{M}} \\ &\quad - V_{\text{SMR}}^{\text{ac,II}} \sin^3 \varphi\left(1 - \sin^2 \varphi \sin^2 \theta_{\text{M}}\right)\cos \theta_{\text{M}} \sin 2\theta_{\text{M}} \\ &\quad - V_{\text{SMR}}^{\text{ac,III}} \sin \varphi \sin 2\varphi\left(1 - \sin^2 \varphi \sin^2 \theta_{\text{M}}\right) \sin 2\theta_{\text{M}} \end{aligned} \tag{6}$$

where $V_{\text{SMR}}^{\text{ac,N}} = \left(\nu_{\text{SMR}}^{\text{ac}}/\nu_{\text{SP}}\right)V_{\text{SP}}^{\text{N}}$ (N=I, II, III) and

$$\nu_{\text{SMR}}^{\text{ac}} = \frac{1}{8}L\rho\frac{\hbar\omega_a}{2|e|d_N\rho}\theta_{\text{SH}}^3\frac{\lambda}{d_N} \tanh\left(\frac{d_N}{2\lambda}\right)(\text{Re } \eta)^2.$$

While the SMR rectified ISHE of ac spin pumping has a different field-angle dependence by the factor $1 - \sin^2 \varphi \sin^2 \theta_{\text{M}}$, the contribution to a dc voltage is week because of $\nu_{\text{SMR}}^{\text{ac}} \propto \theta_{\text{SH}}^3$.

4. Summary

We find that assuming a finite imaginary part of the spin-mixing conductance G_i at the interface between YIG and Pt is helpful in interpreting ST-FMR signals. The ST-FMR line-shape in YIG|Pt bilayers is found to depend sensitively on G_i as well as a phase shift δ between currents and Oersted fields for sufficiently thin YIG layers. Both parameters are strongly correlated and it is difficult to determine them independently by a line-shape analysis. When $\delta=0$, G_i is found to be negative and $\left|G_i\right| \lesssim 0.3G_r$, indicating considerable effective fields that can only be ascribed to the spin–orbit interaction. In order to draw harder conclusions, direct measurement of the phase shift appears indispensible. A promising technique is time-resolved anomalous Nernst effect microscopy that has recently been employed to measure the spatial variation of the relative phase of the Oersted vs. applied ac current across a uniform channel [27]. The previously disregarded rectified ac component of the spin pumping current has a different field-angle dependence than other contributions, but is small since $\sim\theta_{\text{SH}}^3$.

Acknowledgements

We would like to thank Michael Schreier and Ryo Iguchi for valuable discussions. This work was supported by KAKENHI (Grants-in-Aid for Scientific Research) Nos. 22540346, 25247056, 25220910, and 268063, FOM (Stichting voor Fundamenteel Onderzoek der Materie), EU-FET grant InSpin 612759, and DFG Priority Programme 1538 “Spin-Caloric Transport” (Grant no. BA 2954/2).

Appendix A. Field angles dependence of dc voltages

Here we focus on the current-induced magnetization dynamics that generates down-converted dc (and second harmonic) voltages in the NM layer. SMR rectification and spin pumping generate [6]

$$\begin{aligned} V_{\rm dc} &= V_{\rm SMR} + V_{\rm SP} \\ &= \left(V^{\rm I}_{\rm SMR} - V^{\rm I}_{\rm SP}\right)\cos\varphi\ \sin 2\varphi\ \sin\theta_{\rm M} \\ &\quad + \left(V^{\rm II}_{\rm SMR} - V^{\rm II}_{\rm SP}\right)\sin^3\varphi\ \cos\theta_{\rm M}\ \sin 2\theta_{\rm M} \\ &\quad + \left(V^{\rm III}_{\rm SMR} - V^{\rm III}_{\rm SP}\right)\sin\varphi\ \sin 2\varphi\ \sin 2\theta_{\rm M} \end{aligned} \tag{A.1}$$

with

$$\begin{aligned} V^{\rm I}_{\rm SMR} &= v_{\rm SMR}\frac{Cb^r_{ST} + C_+ b_{0e}\ \sin\delta}{\alpha\omega_a/\gamma}F_S(B) \\ &\quad + v_{\rm SMR}\frac{C_+\left(b_{0e}\ \cos\delta + b^i_{ST}\right)}{\alpha\omega_a/\gamma}F_A(B), \end{aligned} \tag{A.2a}$$

$$\begin{aligned} V^{\rm II}_{\rm SMR} &= v_{\rm SMR}\frac{Cb^r_{ST} + C_- b_{0e}\ \sin\delta}{\alpha\omega_a/\gamma}F_S(B) \\ &\quad + v_{\rm SMR}\frac{C_-\left(b_{0e}\ \cos\delta + b^i_{ST}\right)}{\alpha\omega_a/\gamma}F_A(B), \end{aligned} \tag{A.2b}$$

$$V^{\rm III}_{\rm SMR} = v_{\rm SMR}\frac{(C_+ - C_-)b^r_{ST}}{2\alpha\omega_a/\gamma}F_A(B) \tag{A.2c}$$

and

$$\begin{aligned} V^{\rm I}_{\rm SP} &= v_{\rm SP}C\left[\frac{C_-(b^r_{ST})^2 + 2Cb_{0e}h^r_{ST}\ \sin\delta}{(\alpha\omega_a/\gamma)^2}\right. \\ &\quad \left. + \frac{C_+\left(b^2_{0e} + 2b_{0e}b^i_{ST}\ \cos\delta + (b^i_{ST})^2\right)}{(\alpha\omega_a/\gamma)^2}\right]F_S(B), \end{aligned} \tag{A.3a}$$

$$\begin{aligned} V^{\rm II}_{\rm SP} &= v_{\rm SP}C\left[\frac{C_+(b^r_{ST})^2 + 2Cb_{0e}b^r_{ST}\ \sin\delta}{(\alpha\omega_a/\gamma)^2}\right. \\ &\quad \left. + \frac{C_-\left(b^2_{0e} + 2h_{0e}h^i_{ST}\ \cos\delta + (b^i_{ST})^2\right)}{(\alpha\omega_a/\gamma)^2}\right]F_S(B), \end{aligned} \tag{A.3b}$$

$$V^{\rm III}_{\rm SP} = v_{\rm SP}\frac{C\left(C_+ - C_-\right)b^r_{ST}\left(b_{0e}\ \cos\delta + b^i_{ST}\right)}{(\alpha\omega_a/\gamma)^2}F_S(B), \tag{A.3c}$$

where

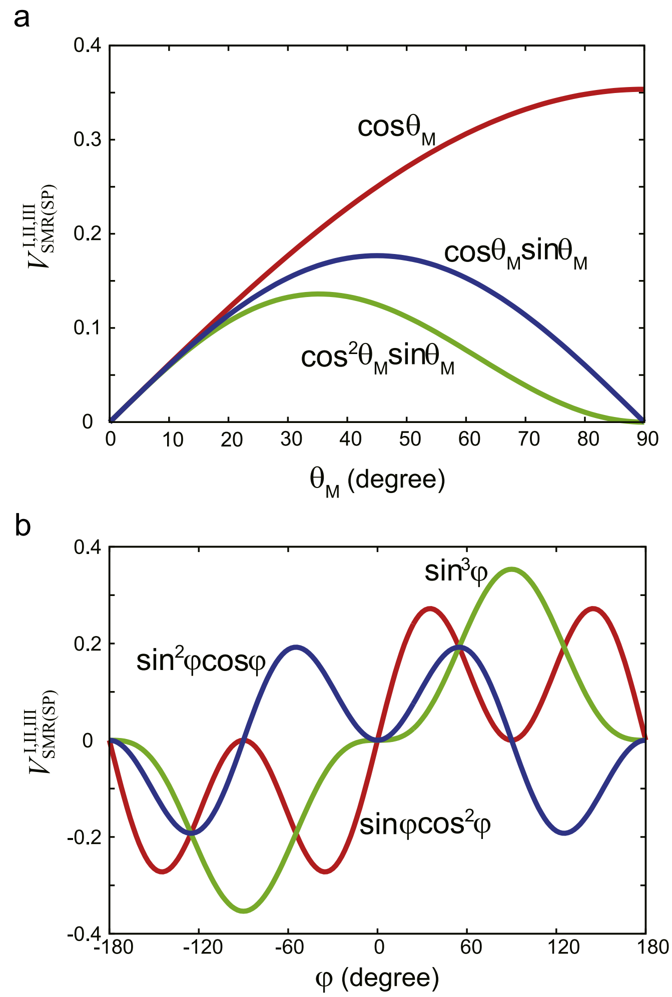

Fig. A1. (a) Polar angle dependence of the dc voltages $V^{\rm I,II,III}_{\rm SMR(SP)}$ with $\varphi=45°$. (b) Azimuth dependence of the dc voltages $V^{\rm I,II,III}_{\rm SMR(SP)}$ with $\theta_{\rm M} = 45°$.

$$v_{\rm SMR} = \frac{1}{4}L\rho J^0_c\theta^2_{\rm SH}\frac{\lambda}{d_N}\ \tanh\left(\frac{d_N}{2\lambda}\right){\rm Re}\ \eta, \tag{A.4a}$$

$$v_{\rm SP} = \frac{1}{4}L\rho\frac{\hbar\omega_a}{2|e|d_N\rho}\theta_{\rm SH}\ {\rm Re}\ \eta, \tag{A.4b}$$

$F_S(B) = \Delta B^2/[(B - B_{\rm R})^2 + \Delta B^2]$, and $F_A(B) = F_S(B)(B - B_{\rm R})/\Delta B$ with the resonance field $B_{\rm R} = \mu_0 M_s\left(\cos 2\theta_{\rm M} + \cos^2\theta_{\rm M}\right)/2 + \sqrt{(\mu_0 M_s\ \sin^2\theta_{\rm M}/2)^2 + (\omega_a/\gamma)^2}/\cos(\theta_{\rm M} - \theta)$ and the FMR linewidth $\Delta B = (\alpha\omega_a/\gamma)/\cos(\theta_{\rm M} - \theta)$, $C = \bar{\omega}_a/\sqrt{1 + \bar{\omega}_a^2}$, and $C_\pm = 1 \pm 1/\sqrt{1 + \bar{\omega}_a^2}$ with $\bar{\omega}_a = 2\omega_a/(\gamma\mu_0 M_s\ \sin^2\theta_{\rm M})$.

The dependence of the dc voltage on applied field directions is shown in Fig. A1 as a function of $\theta_{\rm M}$ and φ.

References

[1] Y. Kajiwara, K. Harii, S. Takahashi, J. Ohe, K. Uchida, M. Mizuguchi, H. Umezawa, H. Kawai, K. Ando, K. Takanashi, S. Maekawa, E. Saitoh, Transmission of electrical signals by spin-wave interconversion in a magnetic insulator, Nature 464 (2010) 262, http://dx.doi.org/10.1038/nature08876.
[2] K. Uchida, J. Xiao, H. Adachi, J. Ohe, S. Takahashi, J. Ieda, T. Ota, Y. Kajiwara, H. Umezawa, H. Kawai, G.E.W. Bauer, S. Maekawa, E. Saitoh, Spin seebeck insulator, Nat. Mat. 9 (2010) 894, http://dx.doi.org/10.1038/nmat2856.
[3] L. Liu, T. Moriyama, D.C. Ralph, R.A. Buhrman, Spin-torque ferromagnetic resonance induced by the spin Hall effect, Phys. Rev. Lett. 106 (2011) 036601,

http://dx.doi.org/10.1103/PhysRevLett.106.036601.

[4] K. Kondou, H. Sukegawa, S. Mitani, K. Tsukagoshi, S. Kasai, Evaluation of spin Hall angle and spin diffusion length by using spin current-induced ferromagnetic resonance, Appl. Phys. Express 5 (2012) 073002, http://dx.doi.org/10.1143/APEX.5.073002.

[5] T. Chiba, G.E.W. Bauer, S. Takahashi, Current-induced spin torque resonance of magnetic insulators, Phys. Rev. Appl. 2 (2014) 034003, http://dx.doi.org/10.1103/PhysRevApplied.2.034003.

[6] T. Chiba, M. Schreier, G.E.W. Bauer, S. Takahashi, Current-induced spin torque resonance of magnetic insulators affected by field-like spin–orbit torques and out-of-plane magnetizations, J. Appl. Phys. 117 (2015) 17–715, http://dx.doi.org/10.1063/1.4913632.

[7] H. Nakayama, M. Althammer, Y.-T. Chen, K. Uchida, Y. Kajiwara, D. Kikuchi, T. Ohtani, S. Geprägs, M. Opel, S. Takahashi, R. Gross, G.E.W. Bauer, S.T. B. Goennenwein, E. Saitoh, Spin Hall magnetoresistance induced by a nonequilibrium proximity effect, Phys. Rev. Lett. 110 (2013) 206601, http://dx.doi.org/10.1103/PhysRevLett.110.206601.

[8] Y.-T. Chen, S. Takahashi, H. Nakayama, M. Althammer, S.T.B. Goennenwein, E. Saitoh, G.E.W. Bauer, Theory of spin Hall magnetoresistance, Phys. Rev. B 87 (2013) 144411, http://dx.doi.org/10.1103/PhysRevB.87.144411.

[9] R. Iguchi, K. Sato, D. Hirobe, S. Daimon, E. Saitoh, Effect of spin Hall magnetoresistance on spin pumping measurements in insulating magnet/metal systems, Appl. Phys. Express 7 (2014) 013003, http://dx.doi.org/10.7567/APEX.7.013003.

[10] M. Schreier, T. Chiba, A. Niedermayr, J. Lotze, H. Huebl, S. Geprğs, S. Takahashi, G.E.W. Bauer, R. Gross, S.T.B. Goennenwein, Current-induced Spin Torque Resonance of a Magnetic Insulator, ArXiv e-prints, arXiv:1412.7460. abs/1412.7460 , 2014.

[11] J. Sklenar, W. Zhang, M.B. Jungfleisch, W. Jiang, H. Chang, J.E. Pearson, M. Wu, J. B. Ketterson, A. Hoffmann, Driving and Detecting Ferromagnetic Resonance in Insulators with the Spin Hall Effect, ArXiv e-prints, arXiv:1505.07791. abs/1505.07791, 2015.

[12] Y. Tserkovnyak, A. Brataas, G.E.W. Bauer, B.I. Halperin, Nonlocal magnetization dynamics in ferromagnetic heterostructures, Rev. Mod. Phys. 77 (2005) 1375, http://dx.doi.org/10.1103/RevModPhys.77.1375.

[13] X. Jia, K. Liu, K. Xia, G.E.W. Bauer, Spin transfer torque on magnetic insulators, Europhys. Lett. 96 (2011) 17005, http://dx.doi.org/10.1209/0295-5075/96/17005.

[14] M. Weiler, M. Althammer, M. Schreier, J. Lotze, M. Pernpeintner, S. Meyer, H. Huebl, R. Gross, A. Kamra, J. Xiao, Y.-T. Chen, H. Jiao, G.E.W. Bauer, S.T. B. Gönnenwein, Experimental test of the spin mixing interface conductivity concept, Phys. Rev. Lett. 111 (2013) 176601, http://dx.doi.org/10.1103/PhysRevLett.111.176601.

[15] C. Du, H. Wang, F. Yang, P.C. Hammel, Enhancement of pure spin currents in spin pumping $Y_3Fe_5O_{12}$/Cu/Metal trilayers through spin conductance matching, Phys. Rev. Appl. 1 (2014) 044004, http://dx.doi.org/10.1103/PhysRevApplied.1.044004.

[16] J. Kim, J. Sinha, S. Mitani, M. Hayashi, S. Takahashi, S. Maekawa, M. Yamanouchi, H. Ohno, Anomalous temperature dependence of current-induced torques in CoFeB/MgO heterostructures with Ta-based underlayers, Phys. Rev. B 89 (2014) 174424, http://dx.doi.org/10.1103/PhysRevB.89.174424.

[17] C.-F. Pai, M.-H. Nguyen, C. Belvin, L.H.V. Leão, D.C. Ralph, R.A. Buhrman, Enhancement of perpendicular magnetic anisotropy and transmission of spin-Hall-effect-induced spin currents by a Hf spacer layer in W/Hf/CoFeB/MgO layer structures, Appl. Phys. Lett. 104 (2014) 082407, http://dx.doi.org/10.1063/1.4866965.

[18] N. Vlietstra, J. Shan, V. Castel, J. ben Youssef, G.E.W. Bauer, B.J. van Wees, Exchange magnetic field torques in YIG/Pt bilayers observed by the spin-Hall magnetoresistance, Appl. Phys. Lett. 103 (2013) 032401, http://dx.doi.org/10.1063/1.4813760.

[19] S. Meyer, R. Schlitz, S. Geprğgs, M. Opel, H. Huebl, R. Gross, S.T. B. Goennenwein, Anomalous Hall effect in YIG|Pt bilayers, Appl. Phys. Lett. 106 (2015) 132402, http://dx.doi.org/10.1063/1.4916342.

[20] M. Harder, Z.X. Cao, Y.S. Gui, X.L. Fan, C.-M. Hu, Analysis of the line shape of electrically detected ferromagnetic resonance, Phys. Rev. B 84 (2011) 054423, http://dx.doi.org/10.1103/PhysRevB.84.054423.

[21] H. Chang, P. Li, W. Zhang, T. Liu, A. Hoffmann, L. Deng, M. Wu, Nanometer-thick Yttrium iron garnet films with extremely low damping, IEEE Magn. Lett. 5 (2014) 6700104, http://dx.doi.org/10.1109/LMAG.2014.2350958.

[22] H.J. Jiao, G.E.W. Bauer, Spin backflow and ac voltage generation by spin pumping and the inverse spin Hall effect, Phys. Rev. Lett. 110 (2013) 217602, http://dx.doi.org/10.1103/PhysRevLett.110.217602.

[23] D. Wei, M. Obstbaum, M. Ribow, C.H. Back, G. Woltersdorf, Spin Hall voltages from a.c. and d.c. spin currents, Nat. Commun. 5 (2013) 3768, http://dx.doi.org/10.1038/ncomms4768.

[24] P. Hyde, D.M.J. Lihui Bai, B.W. Kumar, C.-M. Southern, S.Y. Hu, B.F. Huang, Miao, C.L. Chien, Electrical detection of direct and alternating spin current injected from a ferromagnetic insulator into a ferromagnetic metal, Phys. Rev. B 89 (2014) 180404(R), http://dx.doi.org/10.1103/PhysRevB.89.180404.

[25] C. Hahn, G. de Loubens, M. Viret, O. Klein, V.V. Naletov, J.B. Youssef, Detection of microwave spin pumping using the inverse spin Hall effect, Phys. Rev. Lett. 111 (2013) 217204;
C. Hahn, G. de Loubens, M. Viret, O. Klein, V.V. Naletov, J.B. Youssef, Detection of microwave spin pumping using the inverse spin Hall effect, Phys. Rev. Lett. 112 (2014) 179901, http://dx.doi.org/10.1103/PhysRevLett.111.217204, E.

[26] M. Weiler, J.M. Shaw, H.T. Nembach, T.J. Silva, Phase-sensitive detection of spin pumping via the ac inverse spin Hall effect, Phys. Rev. Lett. 113 (2014) 157204, http://dx.doi.org/10.1103/PhysRevLett.113.157204.

[27] F. Guo, J.M. Bartell, D.H. Ngai, G.D. Fuchs, Phase-sensitive Imaging of Ferromagnetic Resonance Using Ultrafast Heat Pulses, ArXiv e-prints, arXiv:1507.02303. abs/1507.02303, 2015.